THE FLORIDA STATE UNIVERSITY

COLLEGE OF ARTS AND SCIENCES

TEMPORAL AND SPATIAL STRUCTURE OF WIND STRESS CURL OVER THE NORTH ATLANTIC

by

LAURA L. EHRET

A Thesis submitted to the
Department of Meteorology
in partial fulfillment of the
requirements for the degree of
Master of Science

Approved:

James J. O'Brien
Professor Directing Thesis

Jon E. Ahlquist

Steven A. Stage

T. N. Krishnamurti

April, 1986

April, 1986

ABSTRACT

Nineteen years of wind data over the North Atlantic are used to calculate a field of wind stress curl. An EOF analysis is performed on this field resulting in variance-qualified spatial patterns of wind stress curl and associated time series. A Monte Carlo technique is used to establish the statistical significance of each spatial pattern.

The first four statistically significant EOF modes represent more than 50% of the curl variance. The spatial patterns of curl associated with these modes exhibit many elements of North Atlantic climatology. The associated time series are spectrally analyzed. Most of the variance is contained in annual and semiannual frequencies. Features observed include the individual annual variation of the subtropical high and the subpolar low, the annual oscillation of intensity between the above pressure centers, the influence of localized strong SST gradients and associated cyclogenesis regions, and the constant nature of the trades. The EOF curl patterns are in the form of simple standing waves with wavelength on the order of basin size.

ACKNOWLEDGEMENTS

The majority of the work reported herein was done while the author was participating in the NASA Graduate Traineeship in Physical Oceanography and Meteorology.

My first thanks are to Dr. James O'Brien without whose vigor this task would never have been performed, secondly to Dr. Steve Stage for the patient answering of many questions, thanks to Dr. John Ahlquist for being an infinite source, and finally to Dr. T. N. Krishnamurti who made my synoptic experience a pleasure. I am especially grateful to David Legler for his knowledge, encouragement, and enthusiasm.

I thank Rita Kuyper for typing this under overload conditions. I thank my parents, Con and Dorothy, for instilling in me no fear of math and social convention. Finally I wish to note and appreciate the emotional support I received from the other women in meteorology and oceanography here at Florida State.

TABLE OF CONTENTS

LIST OF FIGURES

the variance of wind stress curl. 17

Fig. 6. Same as Fig. 4 for EOF3, corresponds to 8.9% of the variance of wind stress curl. 18

I. INTRODUCTION

The climatology of the atmosphere over the sea is linked to ocean current and sea surface temperature (SST) through the exchange of momentum and heat. It is therefore critical for the modeling of either medium, ocean or atmosphere, to understand the spatial and temporal scales of motion over the ocean. This work addresses that problem over the North Atlantic by applying the technique of empirical orthogonal functions (EOFs).

Other authors have previously estimated statistically the scales of ocean winds. Willebrand (1978) used spectral techniques, considering autospectra and propagation characteristics deduced from cross-spectra. Willebrand recognized the problem of cyclo-stationarity of his data and resolved it through verification of the similiarity of seasonal spectral characteristics. Barnier (1986) used the EOF method for investigating seasonal variability of one specific year of wind stress curl data over the North Atlantic. He questioned whether his results were appropriate for extended times. In this study we use 19 years of data and confirm the similarity of his patterns to those calculated in this study.

Mean wind stress distributions obtained by different methods are available from several sources. Hellerman and

Mean wind stress distributions obtained by different methods are available from several sources. Hellerman and

Rosenstein (1983) used surface wind observations. Using a drag coefficient based on wind magnitude and air-sea temperature difference, they calculate wind stress and wind stress curl on a 2° latitude by 2° longitude grid of global extent. Thompson et al., (1983) calculate wind stress as a function of a monthly mean wind, derived via geostrophy from sea level pressure (SLP), and the seasonal variance of wind as determined from climatology. Willebrand (1978) used SLP maps to derive surface winds and stress from geostrophy and a bulk aerodynamic formula. Bunker (1976) and Leetma and Bunker (1979) use actual ship wind measurements to estimate the mean monthly values of wind on Marsden squares. They subdivided the Marsden squares into 2° latitude by 2° longitude sectors.

The data source for the calculations in this work is the Comprehensive Ocean and Atmosphere Data Set (COADS). The parameter provided by COADS is the measured pseudo-stress parameter, $\bar{u}|\bar{u}|$, where $\bar{u}$ is the velocity vector, centered on 2° latitude by 2° longitude boxes. The curl of the pseudo-stress is calculated at 466 points in the North Atlantic for nineteen years of monthly data. The 466 time series of wind stress curl are combined and statistically resolved in modes representing decreasing amounts of wind stress curl variance. The variance, the spatial distribution of wind stress curl, and a nondimensional time series are associated with each mode. The

the spatial distribution of wind stress curl, and a nondimensional time series are associated with each mode. The spatial distributions are examined for similiarity to climatology. The curl distributions contain patterns indicative

of the oscillation of intensity between the subtropical high and the subpolar low; a second notable pattern can be associated with the region of large sea surface temperature gradient off the coast of North America. The time series are analyzed for annual and interannual variability.

II. DATA DESCRIPTION

The data under consideration are a subset of COADS (Comprehensive Ocean-Atmosphere Data Set). COADS is a global marine data set on a $2^{\circ} \times 2^{\circ}$ grid covering the years 1854 to 1979. The number of reports per month for the Atlantic Basin ranged from less than 5000 during the first 30 years to circa 80,000 in the 1960's and 1970's, the decades herein studied. The collected observations, primarily taken by ships-of-opportunity, are edited and summarized statistically for each month. The COADS variables used are the two wind stress parameters, defined as wind magnitude times the eastward wind component and the northward wind component, respectively. COADS has inherent uncertainties due to historical changes in instrumentation, observation techniques, coding methods, data density, and ship tracking. Specifically, the wind data improved from the transition from estimation from sail and sea state (Beaufort scale) to actual measurement.

The geographical area of the North Atlantic covered by this marine climate study extends from 21°N to 53°N and from 79°W to 11°W. Nineteen years of data were used from January 1961 to December 1979. One hundred and twenty nine near-shore grid blocks were removed to eliminate land effect. Gaps in the data

December 1979. One hundred and twenty nine near-shore grid blocks were removed to eliminate land effect. Gaps in the data

were filled using 8-point spatial interpolation. The vertical component of the curl of the wind stress parameters was then calculated. The temporal mean was calculated and subtracted from all data points. Each of the resulting monthly perturbation wind stess curl sets were subjected to an E-W and a N-S single Hanning filter, i.e. a 1-2-1 running average. At each location the 19-year series of wind stress curl was subjected to a temporal single Hanning filter. These spatial and temporal filters were used to smooth any large jumps between neighboring points that might result from the independent compilation of each of the original data points. The mean and variance fields are shown in Figures 1a and 1b. The mean field compares qualitatively with those of Willebrand (1978), Hellerman and Rosenstein (1983), and Barnier (1986).

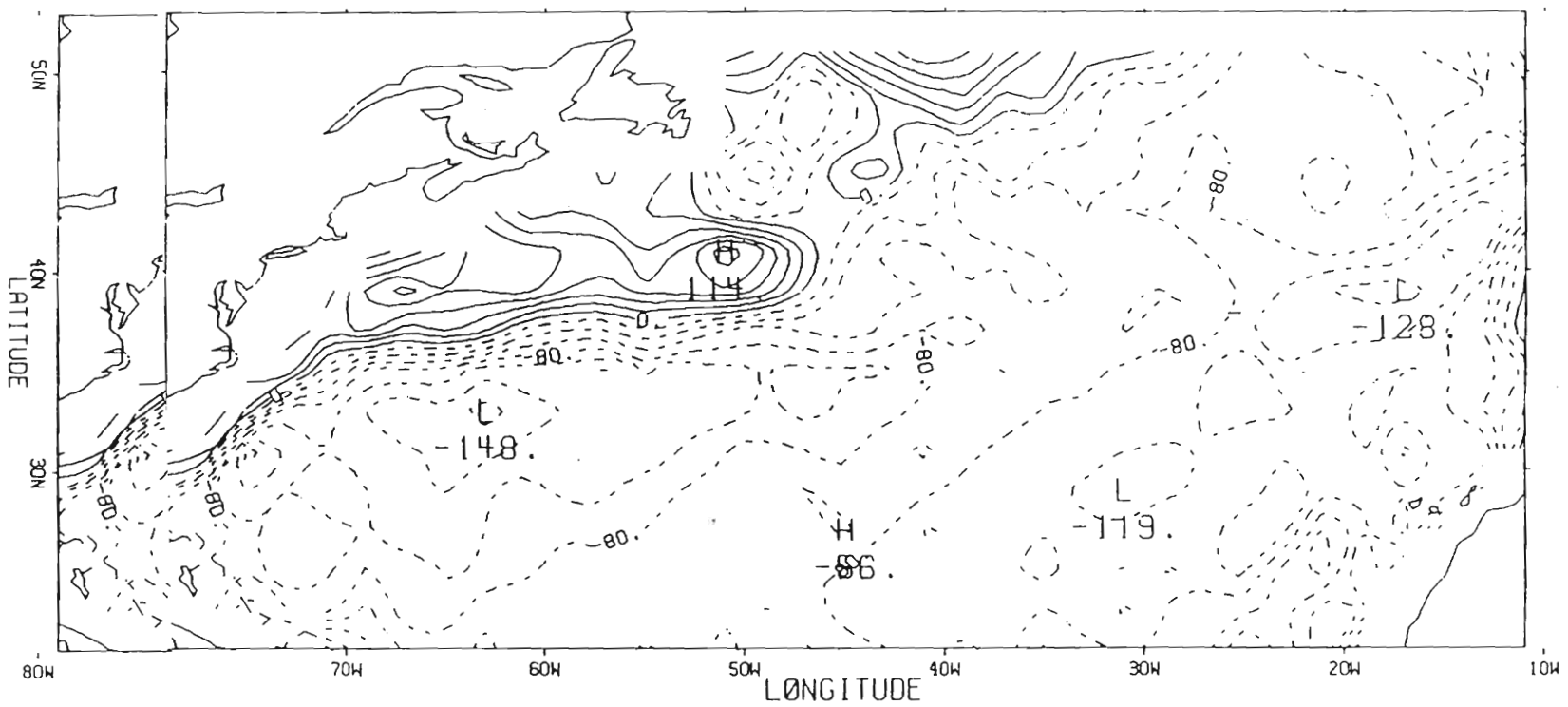

Fig. 1a. Meana. Mean wind stress curl over the North Atlantic from Jan 1961-Dec 1979 (COADS). Dashed line: lines indicate negative curl. Units are $ms^{-2}x\ 10^{-6}$. Contour intervals are 20 $ms^{-2}x\ 10^{-6}$.

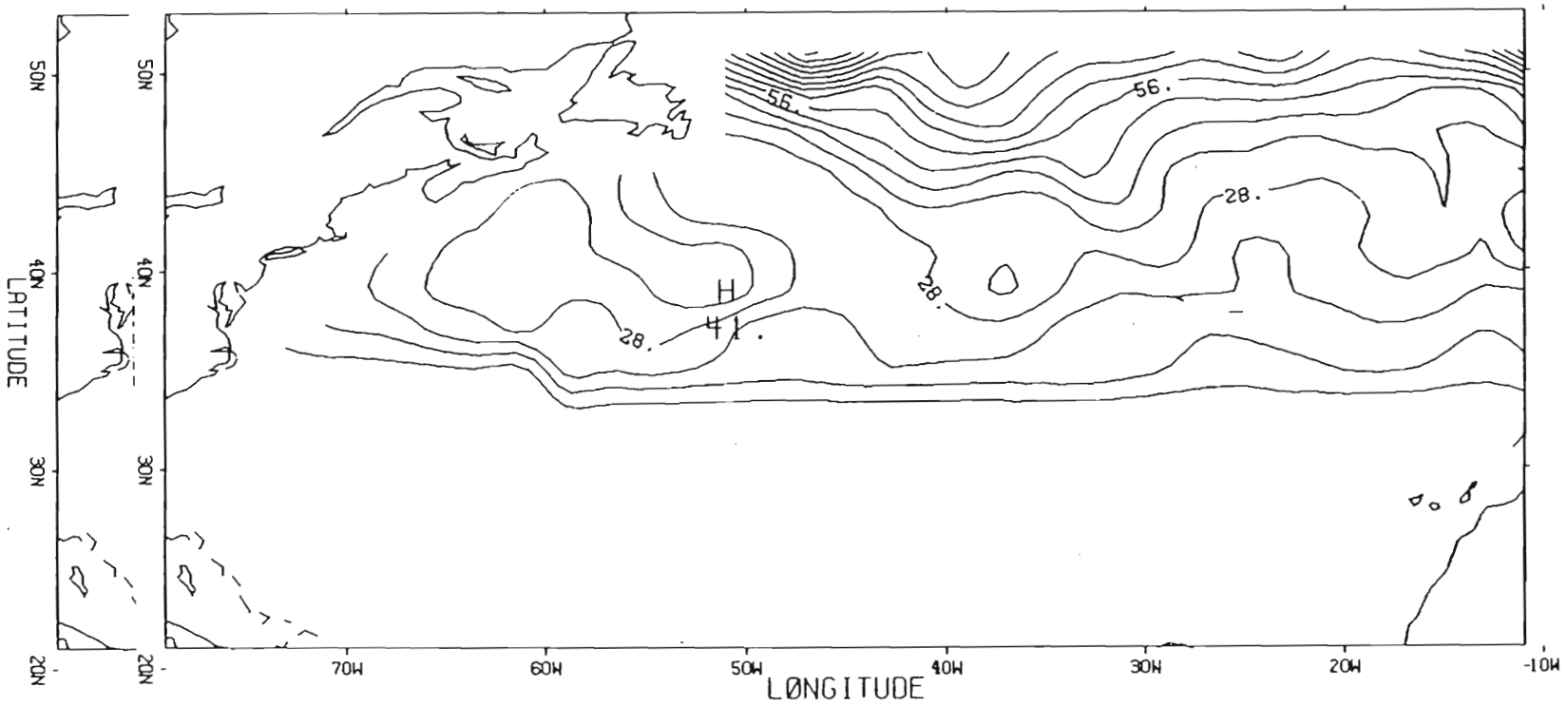

Fig. 1b.ig. 1b. Variance from mean of wind stress curl over the North Atlantic from Jan 1961-Dec 1979 (COADS). Units are $ms^{-2}x\ 10^{-9}$. Contour intervals are 7 $ms^{-2}x\ 10^{-9}$.

III. EOF ANALYSIS

Lorenz (1956) used the eigenvectors of the covariance matrix associated with a sample data field to calculate the coefficients or predictors for a statistical forecasting technique for SLP. Ten years later Kutzbach (1967) reawakened interest in this technique. He calculated statistical relations within and between fields of SLP, surface temperature and precipitation over North America using the same technique as Lorenz. The above technique, called empirical orthogonal function analysis, uses the following general procedure: 1) i sets of real-valued time series $[x_t]$ are formed into an i x n matrix X having i rows corresponding to the number of time series and t columns corresponding to the number of elements in the time series, 2) X is multiplied by its transpose to estimate the i x i spatial covariance matrix, 3) the i eigenvectors of the covariance matrix are used as a basis set, i.e. the original matrix of data can be expressed as a linear combination of the set of eigenvectors, 4) the orthogonality of the eigenvectors and the coefficients of the linear combination is used to solve for the coefficients. The normalized eigenvalue is equal to the percentage of variance represented by the associated eigenvector and its coefficients. The eigenvector of length i is a spatial

percentage of variance represented by the associated eigenvector and its coefficients. The eigenvector of length i is a spatial

distribution of the original data field parameter. The t coefficients are a time series showing the fluctuation of the eigenvector distribution with time.

In the interest of parsimony the above EOF analysis procedure is altered for this work as recommended by the response of von Storch and Hannoschöck (1984) to the work of Legler (1983). Hirose and Kutzback (1969) show that the traditional EOF method and the method used herein produce the same results. The specific procedure applied to wind stress curl over the North Atlantic is described below.

The deviation from the mean of wind stress curl is formed into a 228 x 466 matrix. The 228 corresponds to nineteen years of monthly measurements; the 466 corresponds to the number of spatially distributed stations. From this data matrix a 228-square temporal covariance matrix is calculated by multipling the original array by its transpose. The diagonal elements are variance at time i, where i is the diagonal index. The off-diagonal elements are covariance with lag equal to the difference between the row and column indices. The matrix includes all possible temporal covariance. This symmetric matrix is solved for its 228 real eigenvalues, eigenvectors, and associated coefficients. Each eigenvector is a nondimensional 228-element time series. Each set of coefficients is a 466-point distribution of wind stress curl. When normalized, the eigenvalues are equal to the percentage of total wind stress curl variance associated with each EOF wind stress curl

distribution and its time series.

To illustrate the use of the results of EOF analysis consider a given normalized eigenvalue, its associated spatial distribution of wind stress curl, and time series, λ_A, $C_A(x,y)$, $F_A(t)$, respectively. The distribution $C_A(x,y)$ multiplied by $F_A(t_o)$ represents λ_A percent of the total variance of wind stress curl at time t_o.

Spectra are estimated for the first five time series. The spectral window used has 10.2 degrees of freedom. The frequency-spectra are shown to discern dominant frequencies. A month-by-month average annual signal is calculated and its variance compared to the total variance of the given EOF.

In order to determine if the eigenvalues are above noise level, the EOF procedure was applied to twenty random data sets. These results were used in accordance to the selection rules of Overland and Preisendorfer (1982), to distinguish those eigenvalues attributable to North Atlantic wind from those attributable to a spatially and temporally uncorrelated random process.

IV. RESULTS

Figure 2a and 2b show the distribution of the mean eastward wind stress and the component of wind stress curl associated with eastward stress. Similiarly, Figure 3a and 3b show mean northward wind stress and the distribution of curl associated with northward stress. These mean fields are slightly underestimated. Using $\bar{u}|\bar{u}|$ to represent wind stress corresponds to assuming a linear drag coefficient. In comparision to the usage of an empirical drag formula such as suggested by Large and Pond (1981), the pseudo-stress used in this work greater than 100 m^2/s^2 represents an underestimation. Stress of this magnitude does not appear in the mean stress distributions of Figures 2a and 3a, but does appear in the individual wind data sets. A second cause of underestimation of the mean wind stress curl fields, especially in the higher latitudes, is the use of a Cartesian del operator definition rather than a spherical definition.

By comparing magnitudes and patterns it is obvious that the meridional gradient of the eastward wind stress dominates the total mean wind stress curl, shown in Figure 1. Notable is the thumb of negative curl near Newfoundland, the NE-SW orientation of the pattern near the diagonal and to the east, and the
thumb of negative curl near Newfoundland, the NE-SW orientation of the pattern near the diagonal and to the east, and the

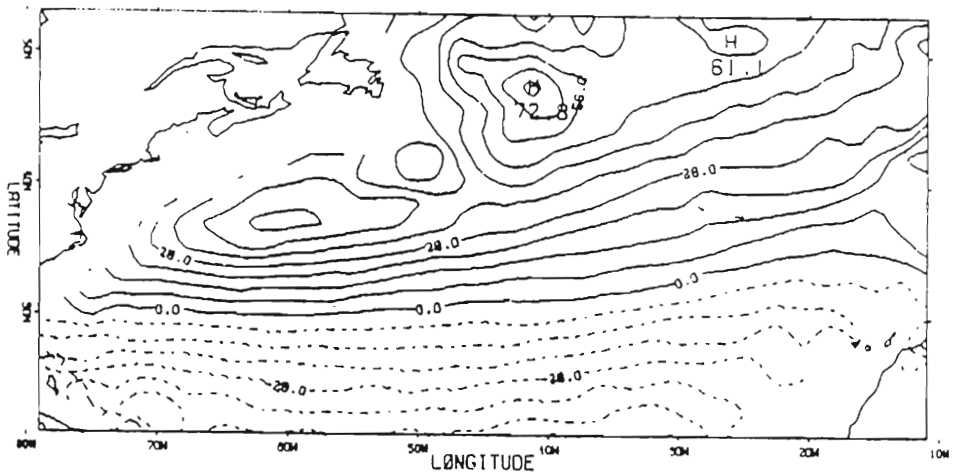

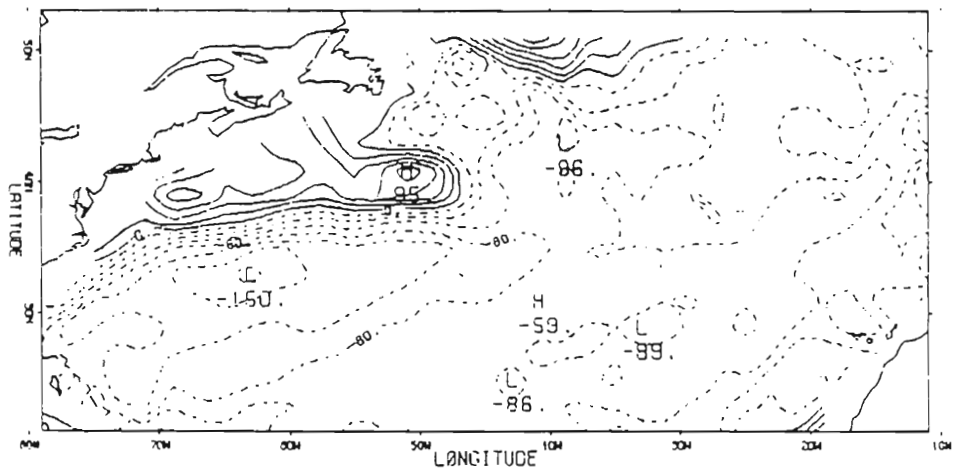

Fig. 2a. Mean eastward wind stress. Dashed lines indicate negative stress. Units are $m^2s^{-2}x10^{-1}$. Contour intervals are 7 m^2s^{-2}.

Fig. 2b. Mean wind stress curl due to the meridional distribution of mean eastward wind stress. Dashed lines indicate negtive curl. Units are $ms^{-2}x\ 10^{-6}$. Contour intervals are

Fig. 2b. Mean wind stress curl due to the meridional distribution of mean eastward wind stress. Dashed lines indicate negtive curl. Units are $ms^{-2}x\ 10^{-6}$. Contour intervals are
20 $ms^{-2}x\ 10^{-6}$.

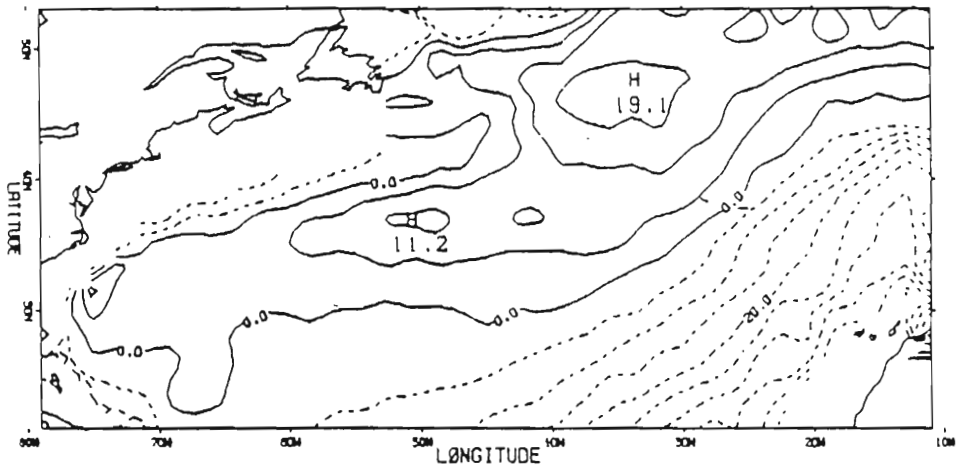

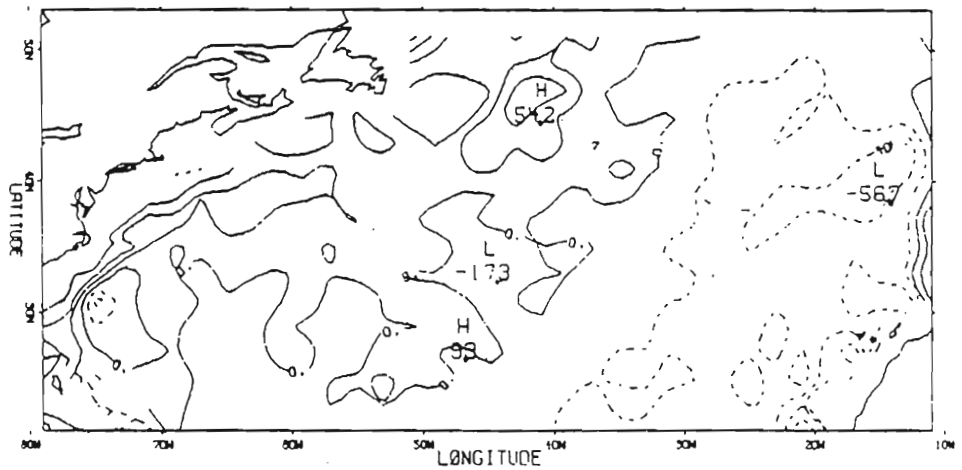

Fig. 3a. Mean northward wind stress. Dashed lines indicate negative stress. Units are $m^2s^{-2}x10^{-1}$. Contour intervals are 5 m^2s^{-2}.

Fig. 3b. Mean wind stress curl due to zonal distribution of mean northward wind stress. Dashed lines indicate negative curl. Units are $ms^{-2}x\ 10^{-6}$. Contour intervals are 20 $ms^{-2}x10^{-6}$

Fig. 3b. Mean wind stress curl due to zonal distribution of mean northward wind stress. Dashed lines indicate negative curl. Units are $ms^{-2}x\ 10^{-6}$. Contour intervals are 20 $ms^{-2}x10^{-6}$

perturbation of this orientation near the North American coast. These characteristics are found also in the results of Willebrand (1979) and Hellerman and Rosenstein (1983). There is a region of maximum curl gradient directly overlying the region of maximum SST gradient at the western ocean boundary. This region of high gradient, which includes a wind stress curl maximum, is mainly due to the eastward stress distribution. The negative curl in the southeast triangle of the field is due to the combined effect of the eastward and northward wind stress distributions.

The synoptic features observable in the mean wind stress curl field are 1) the western basin curl miminum in the region of the Bermuda high, 2) the northern region of positive curl associated with the Greenland low, 3) the relatively constant negative stress in the southern region below 30°N associated with the trade winds.

The variance field is shown in Figure 1b. Wind stress curl variance is constant and small below 30°N. Variance increases with latitude with a local maximum in the region of cyclogenesis near the Canadian coast. The maximum variance gradient in the field is near 50°W, 50°N, due south of Greenland.

The spatial distribution representing the coefficients of the first five EOF's are shown in Figures 4, 5, 6, 7, and 8. The first EOF distribution, Figure 4, contains 24.6% of the
the first five EOF's are shown in Figures 4, 5, 6, 7, and 8. The first EOF distribution, Figure 4, contains 24.6% of the
variance of the wind stress curl. There is a maximum at the center of the North Atlantic basin and a minimum located in the

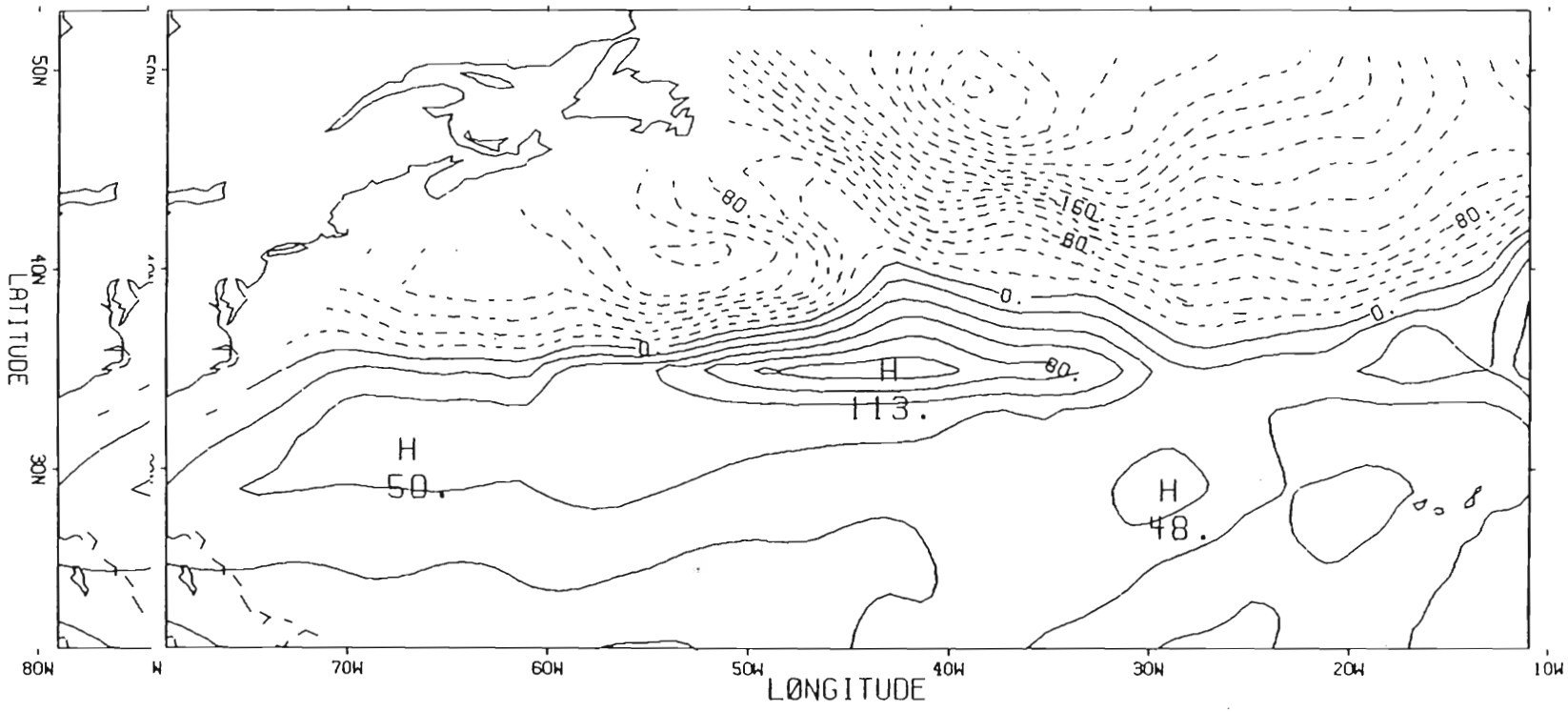

Fig. · Fig. 4. Wind stress curl distribution from EOF1, corresponds to 24.6% of the total variance. Dashed lines represent negative deviation from the mean. Units are $ms^{-2}x10^{-5}$. Contour intervals are 20 $ms^{-2}x10^{-5}$.

northern central part of the basin. Superimposed upon these extrema are an E-W orientation of stress curl lines and a deviation from this orientation near Newfoundland, reminiscent of the thumb of negative curl seen in the mean wind stress curl field. There is small variation below 30°N. The zero lines of the pattern are the nodes of the standing waves that are produced as the spatial pattern is multiplied by the time series. That is, the nodes are those lines which remain fixed as the field oscillates with time. The N-S distribution of EOF1 has a single node around 35°N. The E-W distribution has extrema in the central ocean basin.

EOF2 shown in Figure 5 represents 13.3% of the variance of wind stress curl. There is a single extrema which is negative and located just west of the Azores. The field is dominated by an E-W orientation except for the intrusive effect of the eastern Canadian land mass. There are no nodes in the E-W distribution and a bi-nodal distribution in the N-S with nodes near 45°N and 30°N. Again there is little variation in curl below 30°N.

EOF3 is shown in Figure 6. It represents 8.9% of the variance of the wind stress curl. The EOF3 distribution contains significant zonal variation with a maximum in the western half and a minumum in the eastern half. The latter minimum is centered over the Azores. A second curl low of less

minimum is centered over the Azores. A second curl low of less

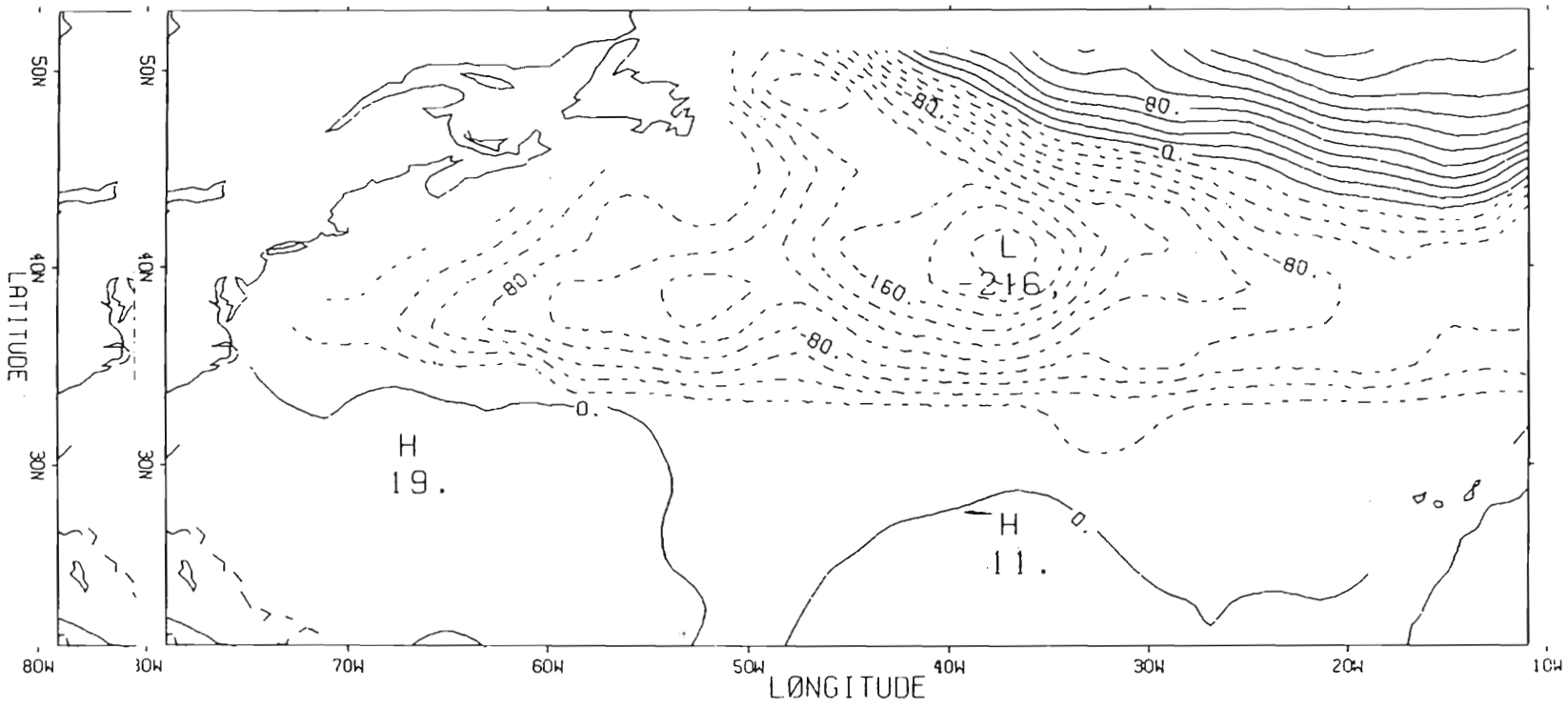

Fig. 5.Fig. 5. Same as Fig.4 for EOF2, corresponds to 13.3% of the variance of wind stress curl.

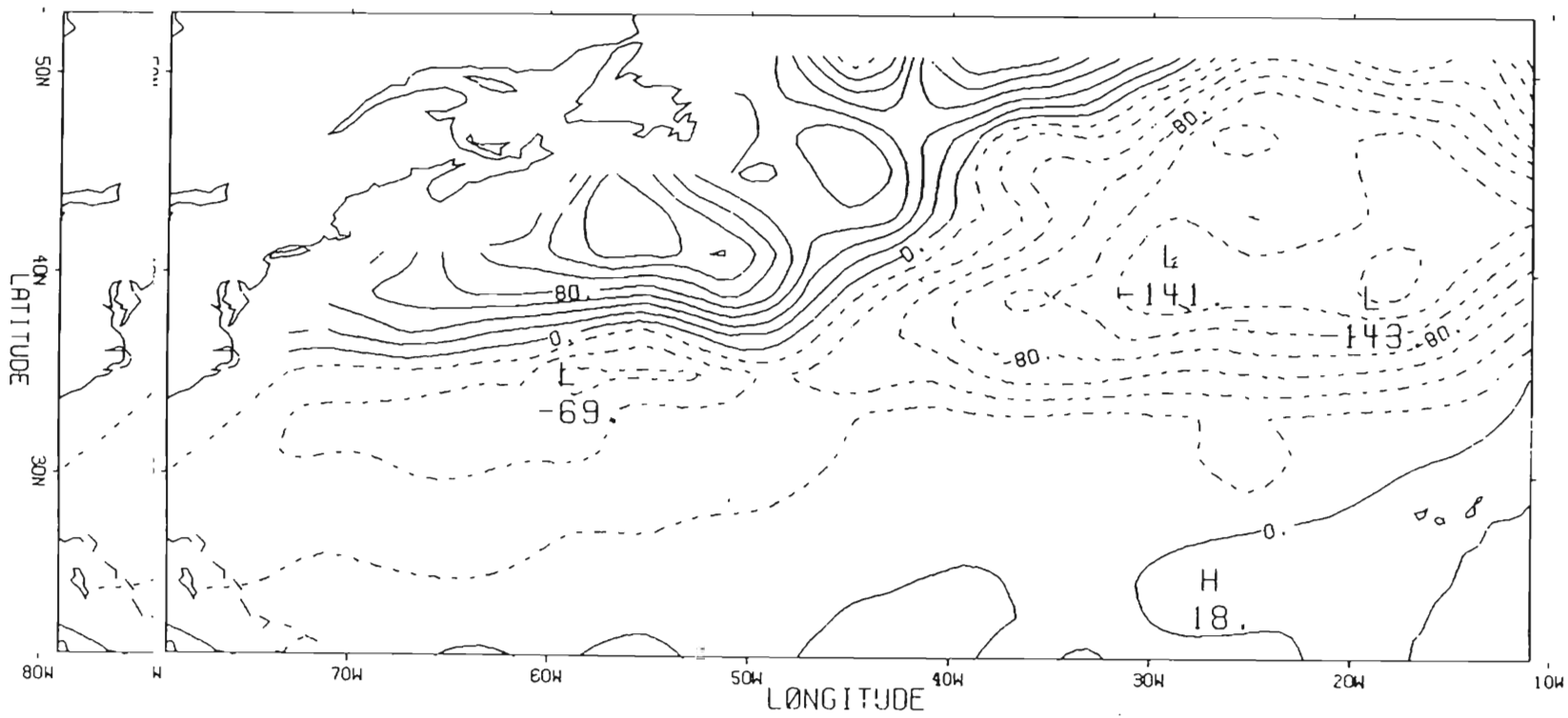

Fig. 6. Fig. 6. Same as Fig.4 for EOF3, corresponds to 8.9% of the variance of wind stress curl.

magnitude is centered over Bermuda. The region along the North American coast is reminiscent of the mean wind stress curl field, i.e. the length of large gradient, the Newfoundland thumb of lesser curl, and the positive curl buildup nearing Greenland. The northern basin is divided by a node line with NE-SW orientation.

EOF4 shown in Figure 7 represents 6.0% of the variance of wind stress curl. The main features of this field are the eastern and western curl maxima of similiar magnitude and separated by a narrow region of slightly negative curl.

EOF5 shown in Figure 8 represents only 4.9% of the variance of wind stress curl. Above 30°N the distribution is clearly divided into four domains with node lines along 30°W and 45°N.

EOF6 and EOF8 (not shown) have irregular distribution allowing no simple characteristic description. EOF7 (not shown) hints of four nodal lines with a NW-SE orientation. The amount of decline between the eigenvalues associated with these three EOF's, is small, a characteristic of the random matrix eigenvalues. These EOF's are not discussed.

The statistical significance of the variance associated with each EOF is verified using the selection rules of Preisendorfer et al., (1981). Twenty sets of eigenvalues are calculated for twenty fields of uncorrelated random numbers. The maxima for each order eigenvalue over these twenty sets

calculated for twenty fields of uncorrelated random numbers. The maxima for each order eigenvalue over these twenty sets

gives the expected eigenvalue limit 95% of the time. To be

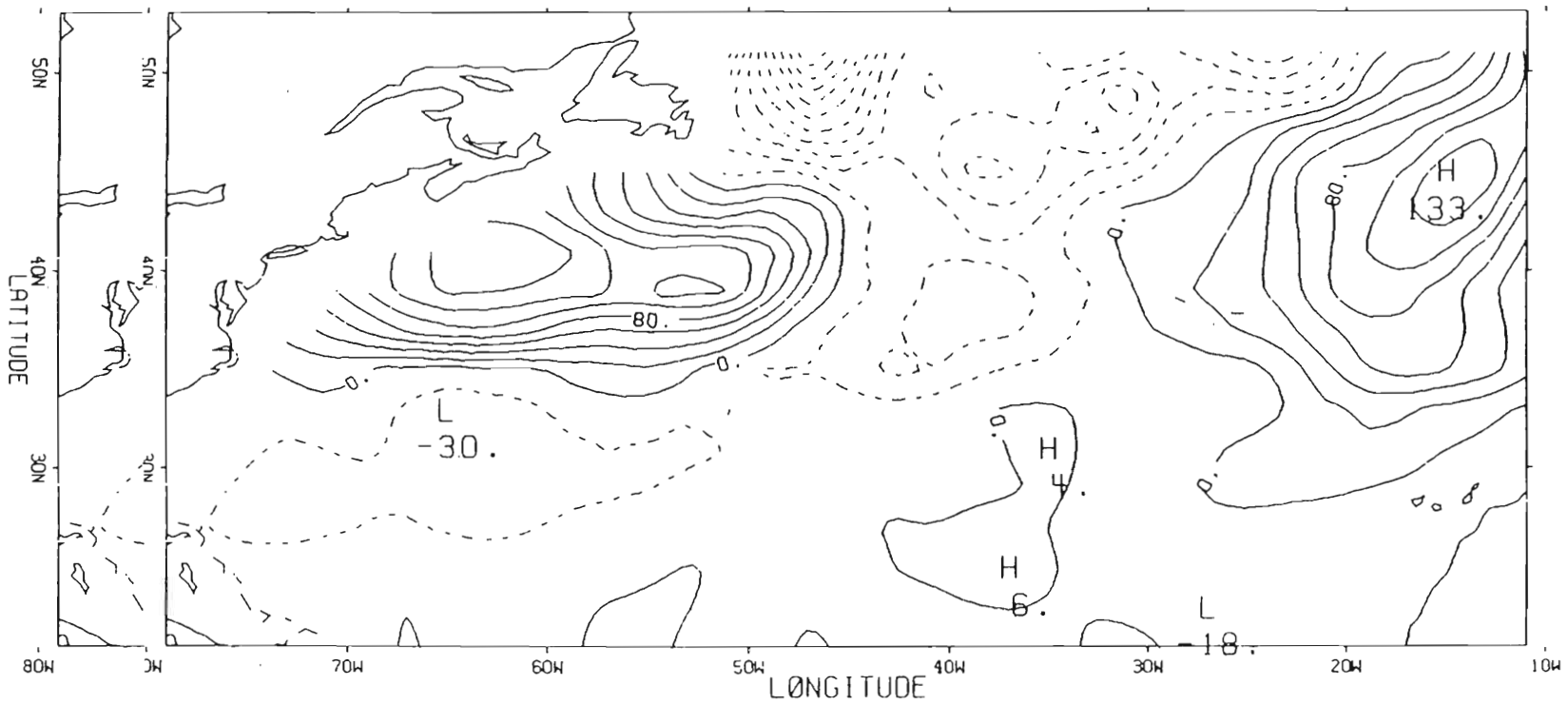

Fig. 7. ig. 7. Same as Fig.4 for EOF4, corresponds to 6.0% of the variance of wind stress curl.

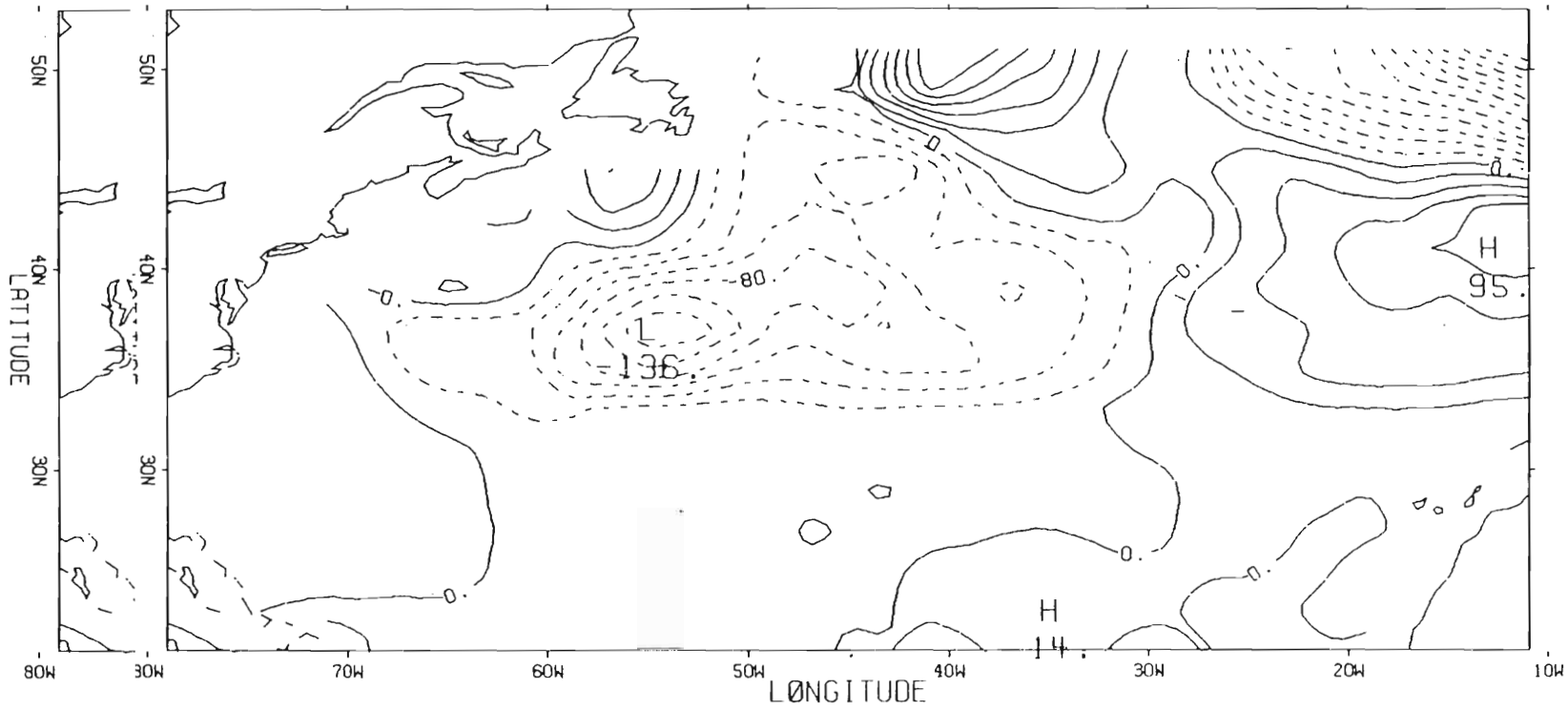

Fig. 8. Fig. 8. Same as Fig.4 for EOF5, corresponds to 4.9% of the variance of wind stress curl.

significant the eigenvalues, or variance, of the North Atlantic wind stress curl field must be significantly greater than the eigenvalues of the uncorrelated field. A table of the first eight eigenvalues of the wind stress curl field and the maximum over the random fields is shown in the following table. This table also shows the cumulative variance and the annual signal percentage of variance of each EOF time series which will be discussed later.

	% Variance (Eigenvalue)	Cumulative % Variance	Random % Variance	Annual % Variance
EOF1	24.61	24.61	1.24	25.05
EOF2	13.26	37.86	1.21	10.31
EOF3	8.92	46.78	1.18	24.40
EOF4	5.99	52.77	1.16	15.29
EOF5	4.89	57.66	1.15	2.32
EOF6	3.59	61.25	1.12	5.58
EOF7	2.92	64.17	1.11	23.02
EOF8	2.25	66.42	1.09	13.13

TABLE 1.

The time series associated with the first five EOF spatial distributions are spectrally analyzed. No tapering is applied. The raw spectra of the first four EOF time series is smoothed using four Hanning passes, producing 10.2 degrees of freedom. Sixteen Hanning passes are used on EOF5. The 90% smoothed using four Hanning passes, producing 10.2 degrees of freedom. Sixteen Hanning passes are used on EOF5. The 90% confidence limits are shown with the log-log spectrum. The

variance preserving frequency-spectrum plot is shown to accent the frequencies most responsible for the time series variance. These results are shown in Figures 9, 10, 11, 12 and 13.

The first EOF time series and its spectra are shown in Figure 9. Superimposed on the time series is the series composite annual signal. The average value for each month is used to form an "expected" year. The composite annual signal is composed of 19 of these expected years. The ratio of the variance of the respective composite annual signal and the variance of all EOF time series is calculated. These values are shown in Table 1. Twenty-five percent of the EOF1 time series is accounted for by the annual signal. The spectrum shows the annual peak as the only peak above the confidence limits. The frequency-spectrum diagram verifies the high level of variance associated with the annual cycle.

The second EOF time series and spectra are shown in Figure 10. The spectrum does not contain any peaks clearly outside the confidence limits. The frequency-spectrum diagram shows the greater part of the variance to be at a near semiannual frequency. There is also an annual peak. The annual signal accounts for 10% of the variance.

The third EOF time series and spectra are shown in Figure 11. This contains a large annual signal ammounting to 24% of the variance. The spectrum contains two significant peak above the confidence limits corresponding to the annual and semiannual frequencies. The frequency-spectrum shows its largest peak of

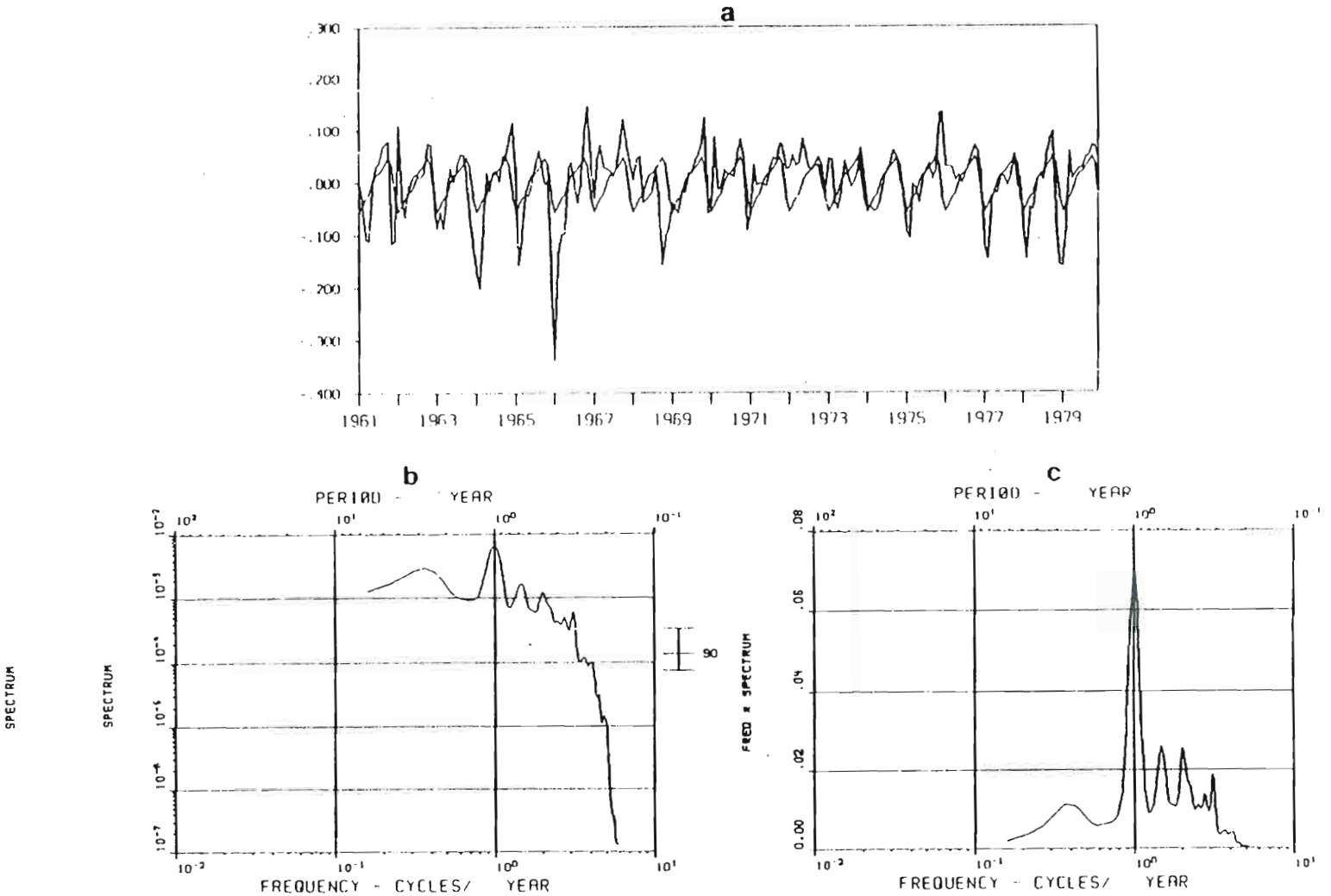

Fig. 9 Fig. 9 (a) Nondimensional time series associated with EOF1. Superimposed is the series annual signal. (b) Spectral estimate using zero tapering and a four Hanning-pass filter; the 90% confidence interval is indicated. (c) Estimated frequency-spectrum.

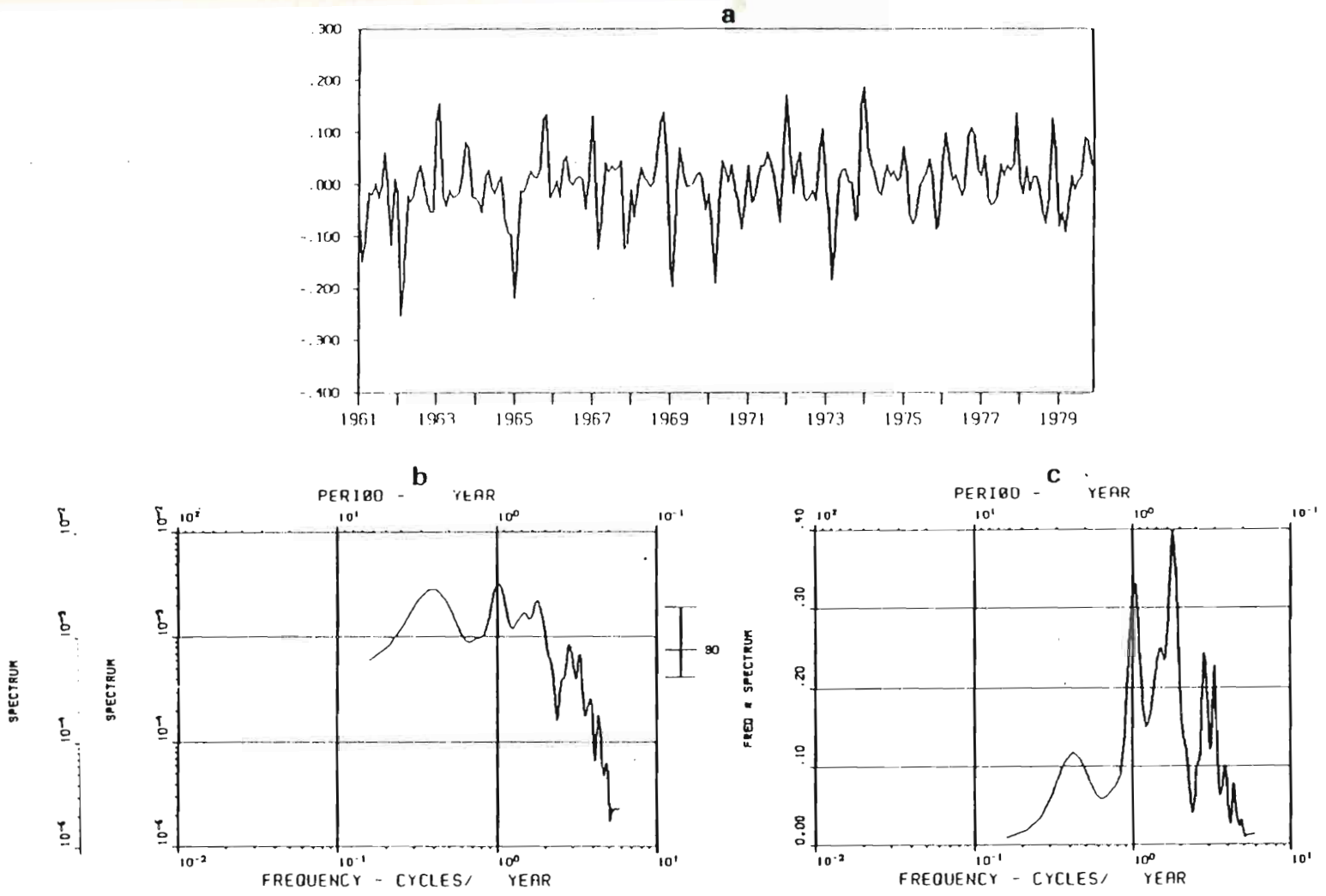

Fig. 10 .g. 10 (a) Nondimensional time series associated with EOF2. (b) Spectral estimate using zero tapering and a four Hanning-pass filter; the 90% confidence interval is indicated. (c) Estimated frequency-spectrum.

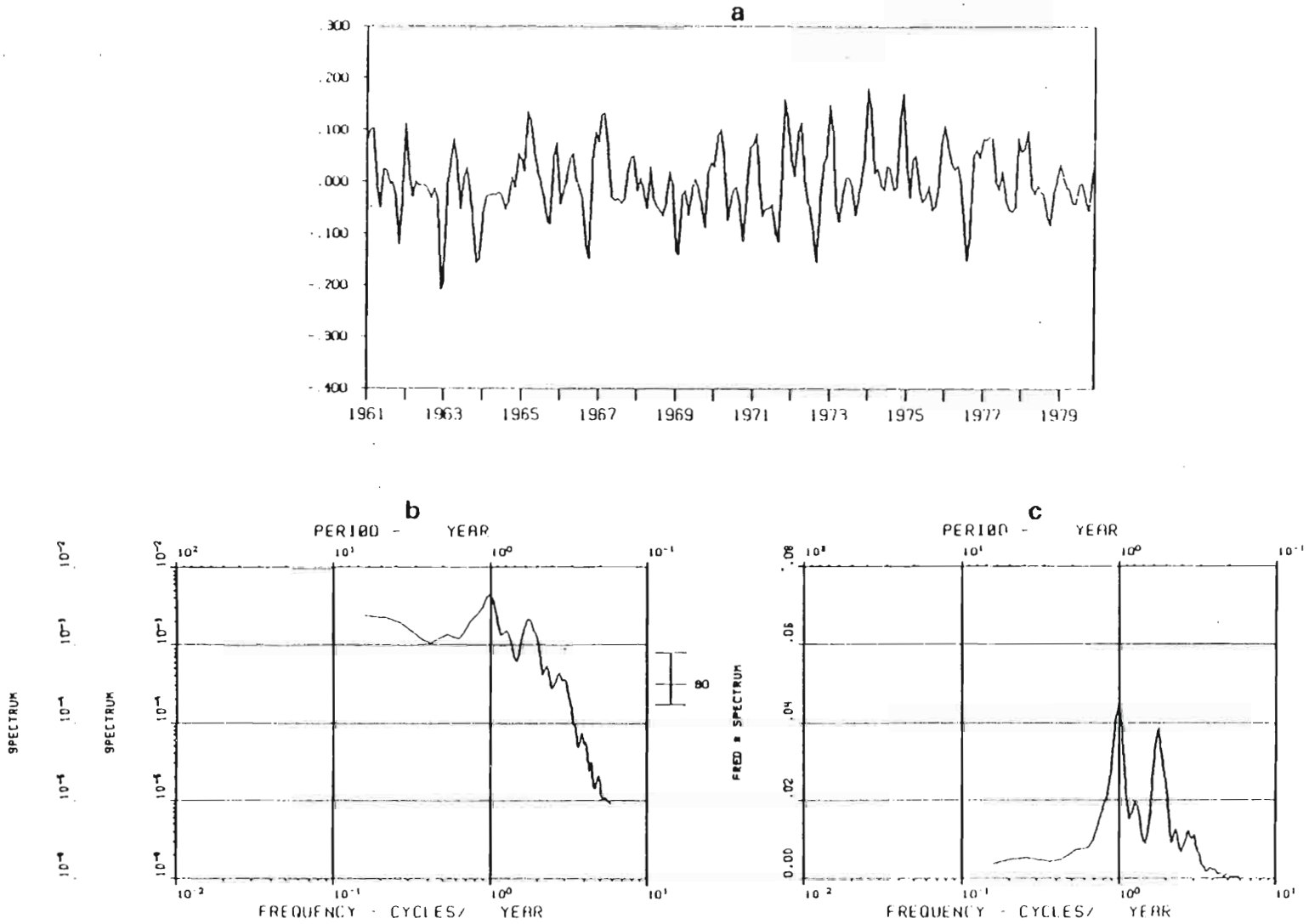

Fig. 11 Same as Fig.10 for EOF3.

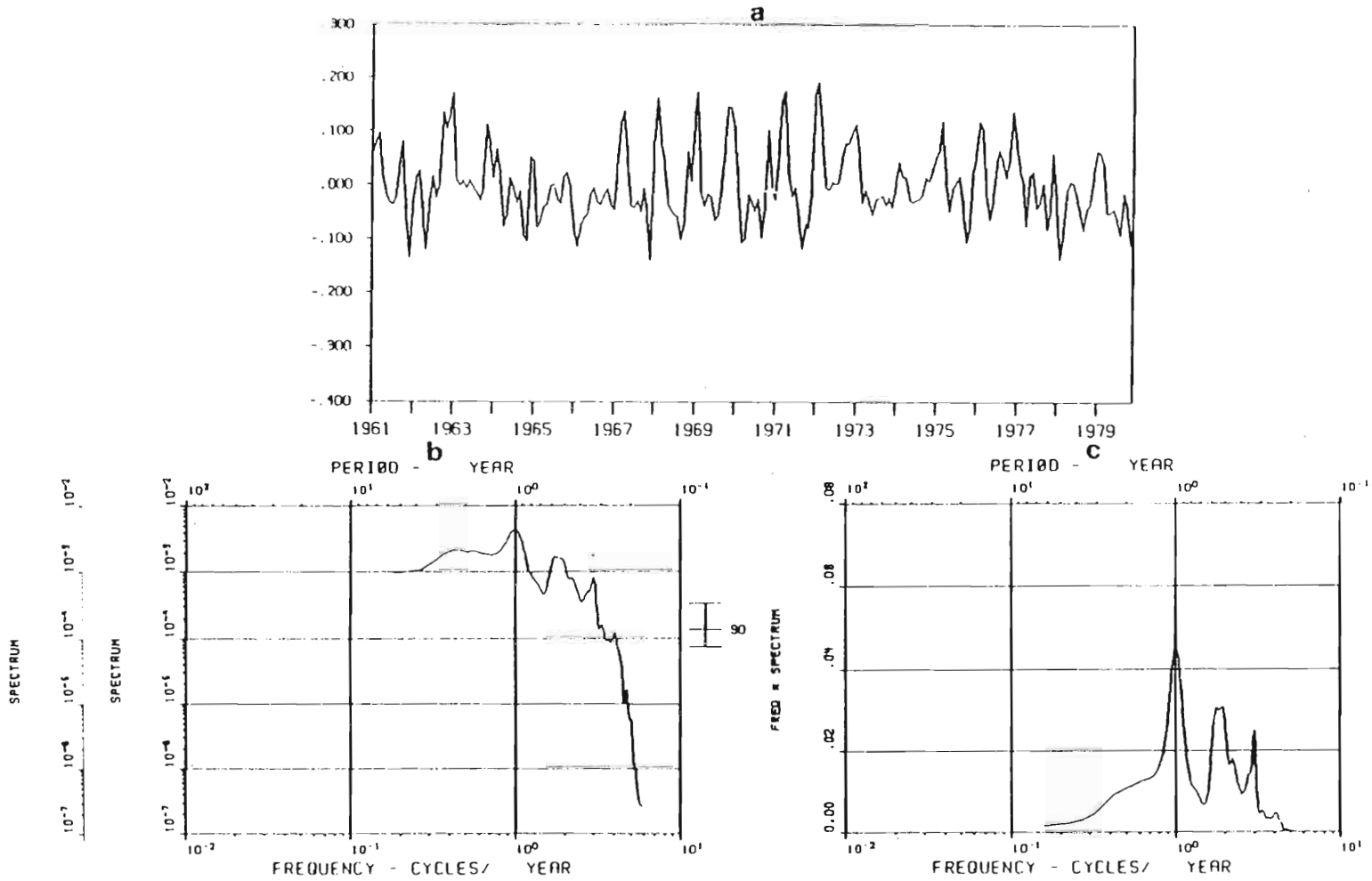

Fig. 12 Same as Fig.10 for EOF4.

variance at the annual frequency and a smaller peak at semiannual frequency.

The fourth EOF time series and spectra are shown in Figure 12. The spectrum shows significant peaks at annual and semiannual frequency with the annual accounting for more of the variance. The annual signal accounts for 15% of the series variance.

The EOF5 time series contains more noise than the previous time series. A spectral estimate with 20 degrees of freedom is used to resolve the variance into dominant frequencies. The fifth EOF time series and spectra are shown in Figure 13. The log-log spectrum shows a significant peak for a period of a third of a year. Variance is mainly distributed between the annual frequency, and a three cycles per year frequency. The annual part of the EOF5 time series accounts for only 2% of the series variance.

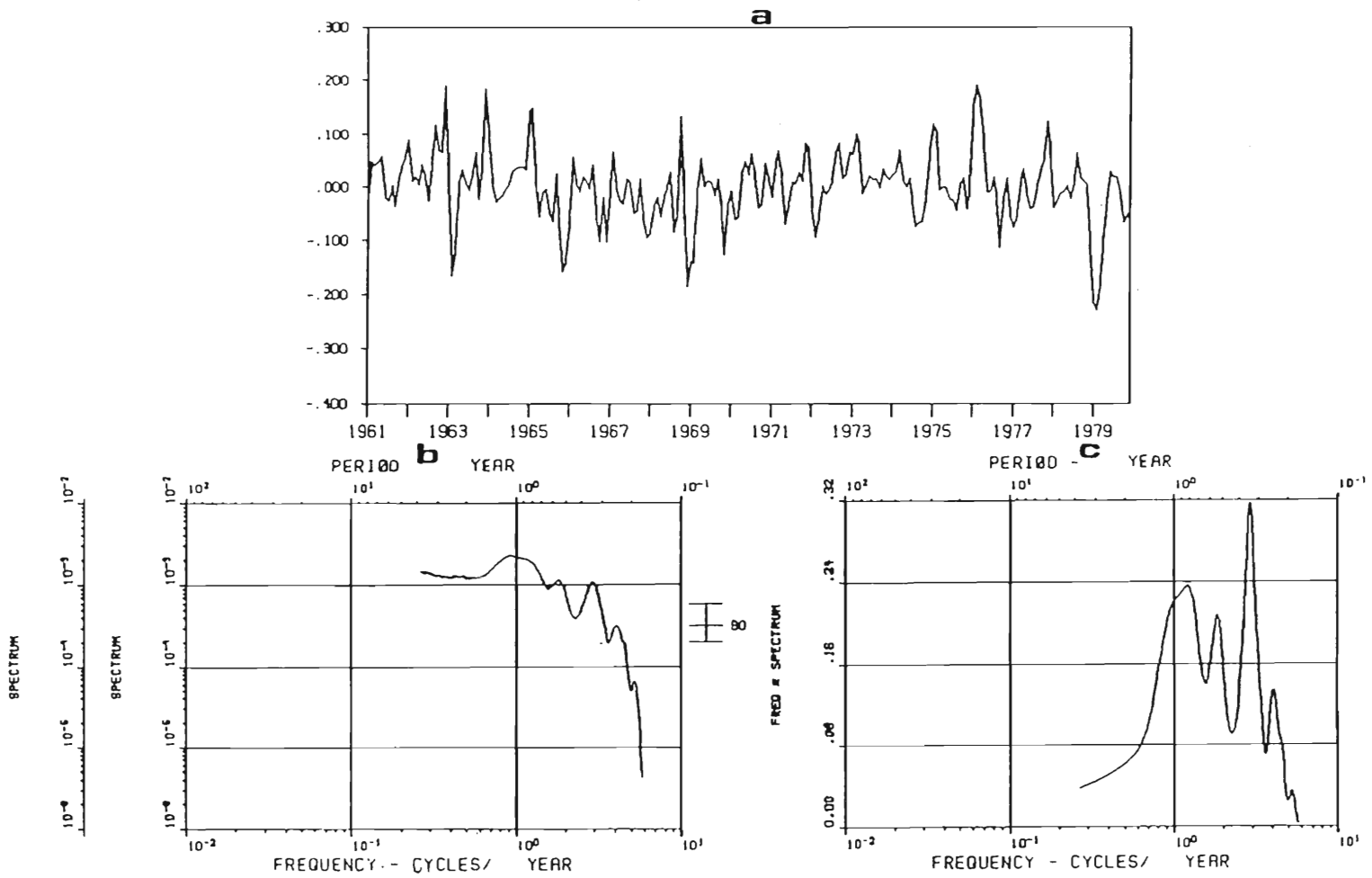

Fig. 13 Same as Fig.10 for EOF5.

V. CONCLUSIONS

The EOF spatial patterns and time series are now examined for geophysical significance. This is done by comparison to features of seasonal circulation known to exist over the North Atlantic. A detailed synopsis of climate over the North Atlantic is available from Tucker and Barry (1984). Elements to consider are: meridional variation of zonal winds with some annual latitudinal variation of position; subtropical high with annual oscillation of position and intensity (maximum in summer); subpolar low with annual oscillation of intensity (maximum in winter); NE-SW orientation of land boundaries; large SST gradient near the coast of North America producing a year-round region of cyclogenesis (maximum intensity in the winter); tropical region of near constant winds with some semiannual variability. Although the curl of the wind stress parameters involves both a wind curl term and a gradient of wind magnitude term, emphasis is placed upon the vorticity term when making physical interpretations, i.e. cyclonic and anticyclonic motion.

The pattern of the first EOF and the strong annual signal of its associated time series implies that much of the variance over the North Atlantic is due to the annual oscillations of intensity of the subpolar low and the subtropical high.
over the North Atlantic is due to the annual oscillations of intensity of the subpolar low and the subtropical high.

Kutzbach (1970), in his Northern Hemisphere study, also found these two areas of opposite anomaly in the North Atlantic. Figure 14 shows the annual signal of the first four EOF time series weighted by $\lambda i/\lambda_1$ where λi is the eigenvalue for the ith EOF. The zeroes of all series are in the temporal proximity of the minimum contrast between the above low and high. The typically negative values of the time series of EOF1 in the winter and the positive values in the summer in conjunction with the EOF1 spatial distribution adhere to the seasonal variation of the subpolar low. The EOF2 spatial distribution and time series imply a decrease of cyclonic motion, or an increase in anticyclonic motion, in the summer in the mid Atlantic and a decrease in anticyclonic motion in the winter. This corresponds to the greater intensity of the subtropical high in the summer. EOF1 and EOF2 distributions appear as meridional standing waves with wavelength slightly larger than the north-south extent of this study. The zonal distribution of EOF2 is a near constant one superimposed on a central minimum; geophysically this is analogous to the meridional gradient of zonal wind superimposed upon the subtropical high.

The third EOF spatial distribution has a zonal and meridional wavelength equal to basin size. EOF3 is dominated by the region of cyclogenesis in the northwest. The EOF3 annual average (Fig. 14) is positive in the winter corresponding to the

the region of cyclogenesis in the northwest. The EOF3 annual average (Fig. 14) is positive in the winter corresponding to the

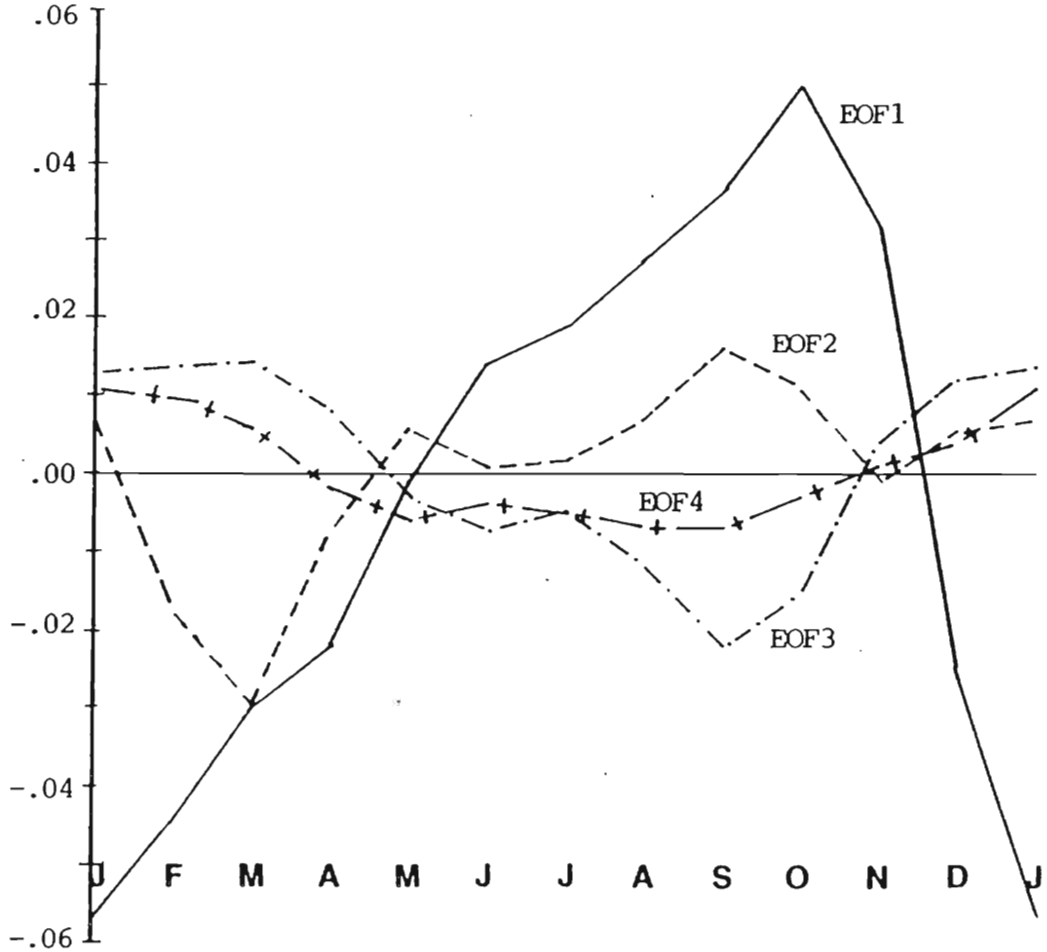

Fig. 14Fig. 14. Overall mean for each month for time series associated with EOF1, EOF2, EOF3, EOF4. The means are weighted by λ_i/λ_1, where λ_i is the eigenvalue associated with EOFi.

greater cyclogenesis in the winter. EOF3 is the first EOF to show the effect of the NE-SW orientation of the land boundaries.

The EOF4 pattern can be interpreted as representing the variance due to blocking highs near Europe. The maximum occurrence of these highs is late spring and autumn for which the time series has negative values. This EOF may represent two geophysical phenomena. Note that the EOF4 western region of positive curl extends into the mid-Atlantic. The EOF4 monthly annual average is positive in the winter (Fig. 14) with a maximum in January. This coincides with the period of maximum extension of large SST gradient into the Atlantic, associated with the increased cyclonic activity.

With its very low annual component, EOF5 does not exhibit any obvious annual climatological features. Of interest is the proximity of the Mid-Atlantic ridge to nodal lines. The zonal standing wave length is approximately basin size. The meridional wave length is slightly larger.

Fifty-eight percent of the wind stress curl variance is contained in patterns clearly exhibiting basin size or greater standing wavelength.

It is seen that time scales associated with the significant EOF's are mostly annual and semiannual; little interannual variability was noted. Thompson et al., (1983) found similiar results. The authors found that the anamolous component (or the

variability was noted. Thompson et al., (1983) found similiar

results. The authors found that the anamolous component (or the nonseasonal component) of wind standard deviation was less than a quarter of the seasonal component 95% of the time. Although

the seasonal dominance was noted, the authors also found that their wind stress induced meridional Sverdurp transport indicated interannual variability upon use of a low pass filter.

Since the annual component of the EOF's is dominant, it is appropriate to compare with Barnier's (1986) one-year study. The three spatial EOF patterns presented by Barnier are similiar to those presented here. The differences are due to the variations of wind in 1979 from the long term mean and, most notably for EOF1, the more northerly extent of Barnier's region to include more of the very active winter storm region near Greenland.

Sorkina (1965) analyzed the SLP over the North Atlantic into six typical patterns. The first four EOF spatial distributions in this study have a correspondent to the geostrophic vorticity fields implied by Sorkina's six patterns.

It is suggested that the propagation features of North Atlantic wind stress curl be studied using Barnett's (1983) EOF method which provides both cospectra and quadrature information. A second suggestion is an EOF analysis of a data set combining COADS wind stress curl and SST. The EOF patterns of North Atlantic SST as calculated by Weare (1977) have points of similiarity with those of wind stress curl.

REFERENCES

Barnett, T. P., 1983: Interaction of the Monsoon and Pacific Trade Wind System at Interannual Time Scales, Part I: The Equatorial Zone. MWR, Vol. 111, 756-773.

Barnier, B., 1986: Analysis of the Seasonal Variability of the Wind-Stress Curl over the North Atlantic Ocean by Means of EOF's. To appear Jan. JGR-Oceans.

Bunker, A. F., 1976: Computation of Surface Energy Flux and Annual Air-Sea Interaction Cycles of the North Atlantic Ocean. MWR, Vol. 104, 1122-1140.

Hellerman, S. and M. Rosenstein, 1983: Normal Monthly Wind Stress over the World Ocean with Error Estimates. J. Phys. Oceanogra., Vol. 13, 1093-1104.

Hirose, M. and J. E. Kutzback, 1969: An Alternate Method for Eigenvector Computations. J. Appl. Met., Vol. 8, Aug., 701.

Kutzbach, J. E., 1967: Empirical Eigenvectors of Sea-level Pressure, Surface Temperature and Precipitation Complexes over North America. J. Appl. Met., Vol. 6, Oct., 791-802.

Kutzbach, J. E., 1970: Large Scale Monthly Mean Northern Hemisphere Anomaly Maps of Sea-level Pressure. MWR, Vol. 98, No. 9, 708-716.

Large and Pond, 1981: Open Ocean Momentum Flux Measurement in Moderate to Strong Winds. J. Phys. Oceanogr., Vol. 11, 324-336.

Legler, D. M., 1983: Empirical Orthogonal Function Analysis of Wind Vectors over the Tropical Pacific Region. Bul. Amer. Met. Soc., Vol. 64, No. 3, 234-241.

Leetma, A. and A. F. Bunker, 1978: Updated Charts of Mean Annual Wind Stress, Convergences in the Ekman Layers, and Sverdrup Transports in the North Atlantic. J. Mar. Res., Vol. 36, 311-322.

Leetma, A. and A. F. Bunker, 1978: Updated Charts of Mean Annual Wind Stress, Convergences in the Ekman Layers, and Sverdrup Transports in the North Atlantic. J. Mar. Res., Vol. 36, 311-322.

Lorenz, E. N., 1956: Empirical Orthogonal Functions and Statistical Weather Prediction. Sci. Rep. No. 1, Stat. Fore. Proj., Dept. Meteor., MIT.

Overland, J. E. and R. W. Preisendorfer, 1982: A Significance Test for Principal Components Applied to a Cyclone Climatology. MWR, Vol. 110, No. 1, 1-4.

Preisendorfer, R. W., F. W. Zwiers and T. P. Barnett, 1981: Foundations of Principal Component Selection Rules. SIO Refer. Series 81-4, UCSD.

Thompson, K. R., R. F. Marsden, and D. G. Wright, 1983: Estimation of Low Frequency Wind Stress over the Open Ocean. J. Phys. Oceanogra., Vol. 13, 1003-1011.

Tucker, G. B. and R. G. Barry, 1984: Climate of the North Atlantic Ocean. Climates of the Ocean, World Survey of Climatology Vol. 15, 193-218, Elsevier Publ.

Von Storch, H. and G. Hannochöck, 1984: Comments on "Empirical Orthogonal Function Analysis of Wind Vectors over the Tropical Pacific Region". AMS Bull., Vol. 65, No. 2, 162.

Weare, B. C., 1977: Empirical Orthogonal Analysis of Atlantic Ocean Surface Temperatures. Quart. J. R. Met. Soc., Vol. 103, 467-478.

Willebrand, J., 1978: Temporal and Spatial Scales of the Wind Field over the North Pacific and North Atlantic. J. Phys. Oceanogra., Vol. 8, 1080-1094.